European Journal of Cardio-Thoracic Surgery 0 (2018) 1–8
doi:10.1093/ejcts/ezy312

REVIEW

Cite this article as: Edlin J, Youssefi P, Bilkhu R, Figueroa CA, Morgan R, Nowell J *et al*. Haemodynamic assessment of bicuspid aortic valve aortopathy: a systematic review of the current literature. Eur J Cardiothorac Surg 2018; doi:10.1093/ejcts/ezy312.

Haemodynamic assessment of bicuspid aortic valve aortopathy: a systematic review of the current literature

Joy Edlin[a], Pouya Youssefi[a], Rajdeep Bilkhu[a], Carlos Alberto Figueroa[b,c], Robert Morgan[d], Justin Nowell[a] and Marjan Jahangiri[a,*]

[a] Department of Cardiothoracic Surgery, St George's Hospital, London, UK
[b] Department of Biomedical Engineering, King's College London, London, UK
[c] Department of Surgery, University of Michigan, Ann Arbor, MI, USA
[d] Department of Radiology, St George's Hospital, London, UK

* Corresponding author. Department of Cardiothoracic Surgery, St George's Hospital, Blackshaw Road, London SW17 0QT, UK. Tel: +44-208-7253565; fax: +44-208-7252049; e-mail: marjan.jahangiri@stgeorges.nhs.uk (M. Jahangiri).

Received 8 June 2018; received in revised form 9 August 2018; accepted 15 August 2018

Key question

Which variables should MRI and CFD investigate in the quest for understanding bicuspid aortic valve (BAV) aortopathy?

Key findings

Flow displacement and wall shear stress are altered in BAV compared to tricuspid aortic valves.

Take-home message

MRI and CFD should focus on wall shear stress for understanding the development and progression of BAV aortopathy

Summary

Both genetic and haemodynamic theories explain the aetiology, progression and optimal management of bicuspid aortic valve aortopathy. In recent years, the haemodynamic theory has been explored with the help of magnetic resonance imaging and computational fluid dynamics. The objective of this review was to summarize the findings of these investigations with focus on the blood flow pattern and associated variables, including flow eccentricity, helicity, flow displacement, cusp opening angle, systolic flow angle, wall shear stress (WSS) and oscillatory shear index. A structured literature review was performed from January 1990 to January 2018 and revealed the following 3 main findings: (i) the bicuspid aortic valve is associated with flow eccentricity and helicity in the ascending aorta compared to healthy and diseased tricuspid aortic valve, (ii) flow displacement is easier to obtain than WSS and has been shown to correlate with valve morphology

and type of aortopathy and (iii) the stenotic bicuspid aortic valve is associated with elevated WSS along the greater curvature of the ascending aorta, where aortic dilatation and aortic wall thinning are commonly found. We conclude that new haemodynamic variables should complement ascending aorta diameter as an indicator for disease progression and the type and timing of intervention. WSS describes the force that blood flow exerts on the vessel wall as a function of viscosity and geometry of the vessel, making it a potentially more reliable marker of disease progression.

Keywords: Bicuspid aortic valve • Aortopathy • Magnetic resonance imaging • Simulation

INTRODUCTION

The bicuspid aortic valve (BAV) affects 2% of the general population, of whom half will undergo cardiac surgery in their lifetime, and in whom aortic dissection is 8 times more likely compared to patients with tricuspid aortic valves (TAVs) [1]. There is variation in clinicians' knowledge of BAV aortopathy, its aetiology and management, as highlighted by Verma *et al.* [2] who surveyed 100 Canadian cardiac surgeons. The discrepancy in the international guidelines [3, 4] contributes to variations in the management of this group of patients. Currently, the timing of prophylactic proximal aortic aneurysm surgery is indicated by the size of the ascending aorta and root. However, many acute aortic events in BAV patients occur at diameters <4.5 cm. In fact, ascending aorta diameter has been shown to be of little importance in predicting acute aortic events in this group of patients [1]. Other factors important in the development and progression of aortopathy in BAV patients include valve morphology and haemodynamic factors.

Magnetic resonance imaging (MRI) and computational fluid dynamics (CFD) are currently being used for functional assessment of patients with normal and diseased BAV. MRI and CFD can be used to calculate haemodynamic variables that explain the development and progression of aortic aneurysm as well as model the effects of surgery. The objective of this review was to summarize the findings of MRI and CFD analyses into BAV aortopathy with particular interest in the variables of flow eccentricity, helicity, flow displacement, cusp opening angle (COA), systolic flow angle, wall shear stress (WSS) and oscillatory shear index (OSI). These variables were chosen because they either influence the blood flow pattern—shown to be altered in both healthy and diseased BAV compared to TAV—or describe the force that blood flow exerts on the aortic wall. WSS acts on the vessel wall and is known to alter its properties, leading to thinning and lumen dilatation. A dissection event, on the other hand, is attributed to tensile stress, a force that acts radially in the vessel wall and is dependent on blood pressure [5]. Current investigations, modelling and computations do not allow for this to be measured easily. Attention is therefore paid to events that precede dissection and rupture.

Histology and genetic theory of bicuspid aortic valve aortopathy

The BAV is associated with intrinsic aortic wall disease, displaying premature cystic medial degeneration in around half of the BAV aortas [6] and reduced fibrillin-1 content independent of valve function [7]. The BAV aortas also have an imbalance in the activity of matrix metalloproteinases (MMPs) and their specific tissue inhibitors. The interplay between MMP activity and TIMP activity impacts on the integrity of the extracellular matrix. This interplay is disturbed in BAV patients leading to increased MMP activity and extracellular matrix degradation. WSS is known to affect MMP activity [8, 9], but there may also be a preprogrammed genetic component to this. The BAV is associated with GATA4 and NOTCH1 mutations [10, 11], but only a small proportion of BAV patients with aortic aneurysm carry these mutations. GATA4 is linked to myocardial differentiation and NOTCH1 codes for a cell surface receptor involved in the development of numerous cell and tissue types. Several other gene mutations have also been implicated in BAV aortopathy [11].

METHODS

A structured review of the literature was performed from January 1990 to January 2018 using the PubMed and MEDLINE databases. The search terms included 'bicuspid aortic valve', 'aortopathy', 'haemodynamics', 'MRI' and 'computer simulation' and combinations thereof using the Boolean operator 'AND'. Once an abstract was identified as useful, the full article was assessed. The references of identified articles were reviewed to detect relevant information and to identify any additional related articles.

Inclusion and exclusion criteria

Studies were included if they referred to the haemodynamic variables such as flow eccentricity and helicity and the associated variables such as flow displacement, COA, systolic flow angle, as well as WSS and OSI in the context of BAV aortopathy. Studies were only included if they derived their results from MRI alone or in combination with CFD and if they were based on human subjects. For example, articles describing CFD simulation based on synthetic models only were excluded.

Studies not published as full-text articles, single case reports, opinion articles and articles not written in English were excluded. No article was excluded based on publication date.

RESULTS

As of 31 January 2018, searches of the databases yielded 310 articles. After exclusion, following the initial screening of the title and abstract, 73 articles were studied in more detail. Following further exclusion, 41 articles remained and are referenced here based on the criteria above. All articles were reviewed by the first author (J.E.) and verified by 2 other authors.

Methods of haemodynamic assessment

CFD simulations require accurate 3-dimensional (3D) geometric models and boundary conditions—data that describe the physical behaviour of the structure under investigation. Three-dimensional geometric models are based on detailed anatomical imaging,

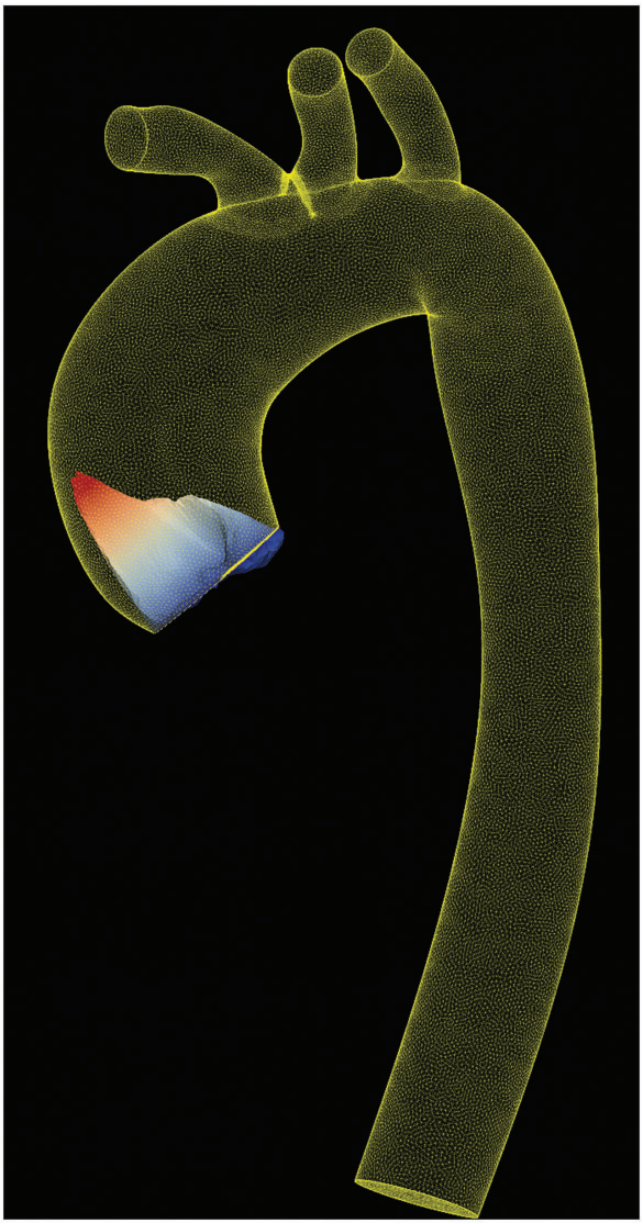

Figure 1: An anatomical mesh constructed using magnetic resonance angiography data with a superimposed velocity profile. The origin of the velocity profile is at the sinotubular junction.

supplied by either cardiovascular MRI or multislice computational tomography. In order to visualize the thoracic aorta in cardiovascular MRI, either MR angiography or high-resolution cardiac- and respiratory-gated 3D steady state in free precision is used. Boundary conditions are derived from phase-contrast MRI, which measures blood flow and velocity at a given plane along the aorta. Finally, the geometric model and boundary conditions are entered into a programme, which computes blood flow simulations, calculating haemodynamic variables throughout the aorta, which can help analyse flow characteristics and biomechanical forces [12] (Fig. 1).

The use of time-resolved 3D phase-contrast MRI, or 4-dimensional (4D) flow MRI, allows measurement and visualization of the spatial and temporal changes of 3D volume. Compared to 2-dimensional (2D) MRI, it produces blood flow velocity data in all dimensions rather than in a given plane. These data are used to calculate WSS. Its application for these purposes has been validated previously [13–15]. Table 1 summarizes the methods for haemodynamic assessment.

Variables used to quantify haemodynamics

Thoracic aorta blood flow pattern in bicuspid aortic valve patients. The visualization of blood flow through MRI and CFD has revealed helical blood flow in BAV patients, with eccentric outflow jet patterns disrupting laminar flow and flow impingement zones along the greater curvature of the ascending aorta [33]. In comparison, non-diseased TAV subjects exhibit a laminar flow pattern in the ascending aorta [34]. Even in the healthy thoracic aorta, blood flow has significant radial components associated with helical flow [13, 35]. This is the result of a combination of ventricular twist and torsion during the systole, the fluid mechanics of the aortic valve and root and the curved geometry of the thoracic aorta [36]. Helical flow has both beneficial and detrimental physiological effects. It is hypothesized that it not only forms a part of normal organ perfusion but also plays a role in plaque deposition and monocyte adhesion, associated with atherosclerosis formation [37].

Bissell *et al.* found 4 patterns of ascending aorta blood flow in a population of 142 subjects, comprising adult and paediatric patients with the normally functioning BAV and stenotic BAV and healthy volunteers with TAV. These were right-handed helical flow and left-handed helical flow, complex flow and normal flow. The most common pattern was the right-handed helical flow, which was associated with larger ascending aorta diameter, higher systolic flow angles and higher rotational flow values compared to healthy volunteers. BAV patients with the normal flow pattern had similar aortic diameters and systolic flow angles to healthy volunteers [38].

They also studied 18 paediatric patients with normally functioning BAVs, of whom one-third already had enlarged ascending aorta diameters and abnormal blood flow patterns. In the remaining two-thirds, 50% had a right-handed helical flow pattern in the ascending aorta, with either a normally functioning or mildly stenotic BAV. This suggests that abnormal blood flow predates aortic dilatation [38].

Flow displacement, flow angle, cusp opening angle and helicity. Parameters used to quantify the degree of helical flow and eccentric flow have been studied in an attempt to describe the changes associated with BAV aortopathy. Flow eccentricity is the deviation of ejected blood in the systole compared to healthy TAV subjects. Parameters that quantify flow eccentricity include flow displacement and flow angle. Flow displacement is defined as 'the distance between the vessel centreline node and the forward velocity-weighted centre of mass position' [39] (Fig. 2). Vector analysis, jet quadrant and flow compression index are alternative ways of describing flow displacement.

COA is the opening angle of each cusp in the systole, an indirect measure of valve stenosis. This determines the systolic flow angle, defined as the angle between the direction of systolic net flow and the unit normal vector (Fig. 3). The sum of both angles equals the unit normal vector. The 2 angles are not haemodynamic parameters *per se*, but they are included as they dictate flow displacement.

Normalized flow displacement has been shown to be a more reliable quantification of flow eccentricity than systolic flow angle

Table 1: Comparison of MRA with CFD and 4D flow MRI

Modalities of haemodynamic assessment	Definition	Application	Advantages	Disadvantages
CFD	Computational simulation of blood flow and calculation of haemodynamics in high spatial and temporal resolution Examples of calculations include the Navier–Stokes equations for blood flow and other calculations of fluid dynamics	To study aneurysms and rupture risk [16–18], the design and evaluation of vascular devices [19] and planning and predicting outcomes of vascular surgery [20, 21]	Can predict behaviour of an aneurysm, vascular device or outcome of surgery without subjecting the patient to that risk [22] Higher spatial resolution than 4D flow MRI [12] and insensitive to phase offsets Can provide information on pressure indices and can account for wall motion via fluid–structure interaction equations [23]	Computationally expensive with simulations lasting 8–12 h Compromised fidelity to reproduce *in vivo* haemodynamics due to assumptions concerning in-flow velocity profiles, blood rheology, choice of turbulence model and parameters, as well as the need for high-quality data for geometry and flow boundary conditions [24, 25] Limitations to modelling of vessel wall characteristic [26]
CMR	Flow measurement is enabled via 2-dimensional PC-MRI to measure blood flow and velocity at a given plane along the aorta	Provides the anatomical data and boundary conditions required to solve equations that yield haemodynamic variables	Shorter scan time than 4D flow MRI Better tolerated by patients	Contrast is required Incorrect placement of acquisition plane can result in underestimation of peak velocities [27] High economic cost
4D flow MRI	3D cine PC-MRI methods are used to derive blood flow velocities in all dimensions	Acquisition of 3D cine PC-MRI with time-resolved ECG-gating and 3D-velocity coding. The technique allows for calculation of 3D phase-contrast angiograms, which in turn provide information on aortic size, and geometry through multiplanar reconstruction [28] allows quantification of flow at any location within a volume [29]	Allows direct measurement of *in vivo* 3D flow velocities Haemodynamic measurements, e.g. WSS, can be calculated from the anatomical and flow data Unaffected by boundary conditions	Contrast is required. Longer scan time Semi-automated data analysis has been developed to reduce analysis time for certain haemodynamic parameters [30] The accuracy of different haemodynamic variables is influenced by the MRI scan protocol [31], resulting in WSS underestimation due to spatial resolution and noise [32]

CFD: computational fluid dynamics; CMR: cardiac magnetic resonance; ECG: electrocardiography; MRA: magnetic resonance angiography; MRI: magnetic resonance imaging; PC-MRI: phase-contrast MRI; WSS: wall shear stress; 3D: 3-dimensional; 4D: 4-dimensional.

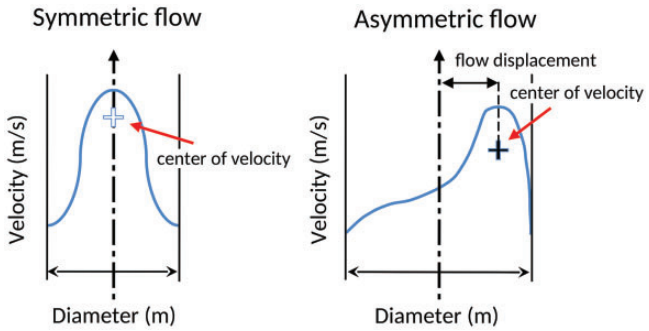

Figure 2: Flow displacement, which is the 'distance between the vessel centreline node and the forwards velocity-weighted centre of mass position' [15].

[40]. It is larger in BAV patients compared to TAV subjects, matched for aortic diameter and valvular function, [33, 41] and correlates with distal ascending aorta diameter in BAV patients with fusion of the right and non-coronary cusps (RN-BAV) but not in BAV patients with fusion of the right and left coronary cusps (RL-BAV) [41]. Flow displacement has also been identified as a potential marker for BAV aortopathy phenotype, showing that both type 1 aortopathy (involvement of the aortic root) and type 3 (the distal ascending aorta) aortopathy are more common in RN-BAV, whereas type 2 aortopathy (the mid-ascending aorta) is more common in RL-BAV [33, 42, 43].

Della Corte *et al.* [44] used the COA to show restricted valve cusp motion in 36 patients with normally functioning BAV compared with 10 healthy volunteers with TAV. In the BAV patients, the conjoined COA was 62°± 5° compared to 76° ± 3° for the non-fused leaflet and 75°± 3° for the TAV cusps, and employing CFD, they showed that a reduced COA is sufficient to cause flow displacement. Bissel *et al.* [38] showed that a reduced COA is associated with a higher positive rotational flow and WSS. These findings explain why a normally functioning BAV displays abnormal blood flow in the ascending aorta compared to healthy TAV. Della Corte *et al.* [44] also showed that COA is inversely proportional to the ascending aorta diameter adjusted for body surface area and to the aortic diameter growth rate. Therefore, the greater the BAV stenosis, the larger the ascending aorta diameter and its growth rate.

Simply visualizing helical flow does not allow quantification of the haemodynamic consequences of BAV morphology or the severity of the valve disease. Helicity describes the relationship between velocity and vorticity of flow, whereas helical flow index quantifies the degree of helicity [45]. Helicity is also described as a positive helix fraction index [46]. Our group has shown that the helical flow index is higher in BAVs compared to diseased and healthy TAVs and that the helical flow index is higher in stenotic

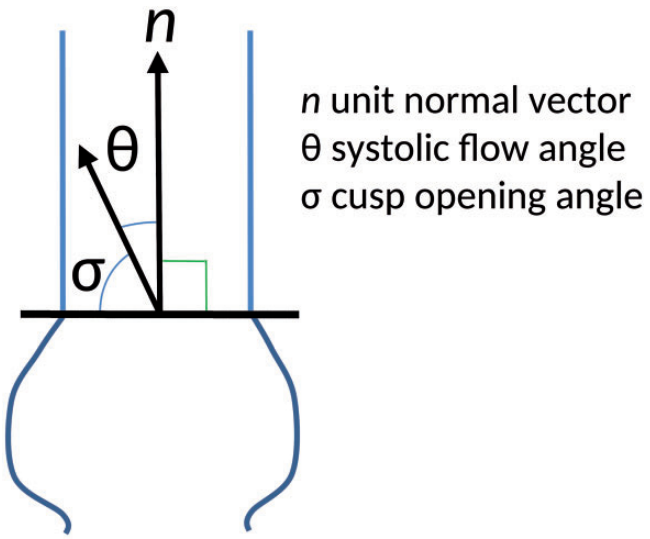

Figure 3: A diagram of cusp opening angle (σ) and flow angle (θ). *n* is the unit normal vector perpendicular to a plane orthogonal to the ascending aorta just distal to the sinotubular junction or through the plane of the sinotubular junction. Some researchers place *n* in the axis of the left ventricular outflow tract.

RL-BAVs compared to stenotic RN-BAVs [47], quantifying how blood flow is affected by BAV morphology. Helicity has also been shown to be proportional to systolic flow angle and WSS [38].

Wall shear stress and oscillatory shear index. WSS refers to the force (N) per unit area (m^2) exerted by a moving fluid in the direction of the local tangent of the tubular surface. Blood viscosity and blood flow profile immediately next to the vessel wall exerts WSS on the endothelium. WSS has been shown to affect expression of transcriptional factors implicated in vascular remodelling, in particular the expression of MMPs [8, 9].

Compared to TAV, BAV has been shown to generate higher and asymmetrically distributed WSS along the greater curvature of the ascending aorta [9, 40, 43, 44], where dilatation and thinning are typically found [48]. This corresponds to patterns of flow displacement [33] and may explain the dilatation pattern seen in the ascending aorta of BAV patients [49]. Shan *et al.* [50] quantified this displacement of WSS by introducing WSS eccentricity threshold, defined as the difference between the WSS in the right-anterior and left-posterior segments of the aorta, WSS_{RA}-WSS_{LP} >0.2 N/m^2, and showed that eccentric WSS distribution was greatest in the stenotic BAV group, followed by the control BAV group and regurgitant BAV group. Moreover, peak systolic WSS has been found to travel in a right-handed helix in both non-stenotic and stenotic RL-BAV patients [38, 51].

The pattern of WSS distribution along the ascending aorta is different in stenotic compared to regurgitant BAV patients. Compared to normally functioning BAV, the WSS is circumferentially elevated in all analysis planes of the ascending aorta in regurgitant BAV [50]. Moreover, WSS is proportional to the mid-ascending aorta diameter in normally functioning BAV and regurgitant BAV. At the same level, WSS is proportional to peak blood flow velocity in stenotic BAV patients [50] and to the degree of BAV stenosis [52]. van Ooij *et al.* [53] found that WSS was proportional to the degree of aortic stenosis and that for moderate and severe aortic stenosis, the relationship between WSS distribution and BAV morphology disappeared.

Malek *et al.* [54] report the atheroprotective level of WSS at >1.5 N/m^2 and deleterious WSS at <0.4 N/m^2. All values of WSS, from the proximal to distal ascending aorta, for BAV and healthy volunteers reported by Mahadevia *et al.* [33] were >0.55 N/m^2 ± 0.16 N/m^2 and >0.56 ± 0.16 N/m^2, respectively, as reported by van Ooij *et al.* [53]. The TAV group matched for aortic size displayed WSS at <0.41 N/m^2 ± 0.16 N/m^2 [33]. Meierhofer *et al.* [55] found a similar median WSS for their healthy volunteers and the normally functioning BAV group. Shan *et al.* [50] calculated WSS as >0.61 N/m^2 ± 0.08 N/m^2 for stenotic and as >0.69 N/m^2 ± 0.15 N/m^2 for regurgitant BAV in the proximal to distal ascending aorta, with the highest values in the mid-ascending aorta. Our group also found elevated values of mean WSS in the mid-ascending aorta of BAV patients compared to healthy volunteers [47] (Table 2).

All WSS values calculated for normally functioning BAV and diseased BAV were >0.4 N/m^2. Calculated WSS for healthy volunteers with TAV were found to be less than 0.4 N/m^2, especially in the series of Shan *et al.* [50] (Table 2).

OSI is a quantification of the change in direction and magnitude of WSS. Both parameters have been shown to be associated with aneurysm formation [56] and vasculopathy [45]. Analogous to the findings of WSS, OSI distribution is only symmetrical in the ascending aorta of healthy volunteers, compared to stenotic TAV and BAV that show varying degrees of asymmetrical OSI during the cardiac cycle. The largest difference in OSI is found in the stenotic RN-BAV group in the sectors corresponding to the greater curvature of the ascending aorta [47].

DISCUSSION

Patients with normally functioning BAV display altered blood flow patterns with an effect on WSS compared to healthy TAV subjects matched for aortic diameter size. These changes are exacerbated in stenotic BAV and regurgitant BAV, supporting a haemodynamic component to the development of BAV aortopathy, whether acting alone or in combination with a genetic predisposition. To cement this association and understand the behaviour of both aneurysm formation and evolution, longitudinal studies of the relevant haemodynamic variables are required. This poses both practical and financial hurdles, to which computer simulation, in the form of CFD, offers a potential solution.

In the past, much attention has been given to aortic diameter, but it has been shown to be a poor indicator of an acute aortic event in the BAV cohort [1, 57]. It is also known that the behaviour of aneurysms cannot be predicted by their largest diameter alone. Their entire geometry, and the presence of atherosclerosis and thrombi also affect their behaviour [58].

Blood flow pattern and flow displacement

Blood flow pattern and flow displacement are easily visualized and calculated with data from either 2D or 4D flow MRI without the need for further extensive computations. Moreover, flow displacement is easier to obtain than WSS [43] and has been shown to correlate BAV morphology with the type of aortopathy [33, 42, 43]. Blood flow pattern and flow displacement are, therefore, helpful parameters to predict how disease progression of the BAV may affect an aortopathic phenotype.

Table 2: Comparison of WSS values reported in the literature

Groups	Modality	Mean WSS (N/m^2) at the mid-ascending aorta		
		Healthy TAV, not matched for ascending aorta diameter	Normally functioning BAV	Diseased BAV
Mahadevia *et al.* [33]	4D flow MRI	0.56 ± 0.14	0.56 ± 0.18, RL-BAV 0.61 ± 0.21, RN-BAV	
Meierhofer *et al.* [55][a]	4D flow MRI	0.48	0.55	
van Ooij *et al.* [53][a]	4D flow MRI	0.56	0.78, RL-BAV[b] 0.73, RN-BAV[b]	0.97, RL-BAV[c] 0.98, RN-BAV[b] Moderate–severe stenosis
Shan *et al.* [50]	4D flow MRI	0.44 ± 0.07	0.57 ± 0.09	0.75 ± 0.12, regurgitant 0.70 ± 0.11, stenotic
Youssefi *et al.* [47]	MRA and CFD	0.98 ± 0.54		2.73 ± 1.0, RL-BAV 3.71 ± 0.4, RN-BAV

[a]Median WSS magnitude, with the resulting net vector along the entire vascular wall.
[b]Along the lesser curvature of the proximal ascending aorta.
[c]Along the greater curvature of the proximal ascending aorta.
BAV: bicuspid aortic valve; CFD: computational fluid dynamics; MRA: magnetic resonance angiography; MRI: magnetic resonance imaging; RL-BAV: right–left coronary cusp BAV fusion pattern; RN-BAV: right-non-coronary cusp BAV fusion pattern; TAV: tricuspid aortic valve; WSS: wall shear stress; 4D: 4-dimensional.

Wall shear stress

WSS has been shown to both affect vessel remodelling on a cellular level and have an impact on atherosclerosis [9, 54]. It has, therefore, been the haemodynamic parameter of choice in investigating vasculopathy in the abdominal, renal and cerebral circulation and now in the thoracic aorta. Several studies show an elevated and asymmetrical distribution of WSS in stenotic BAV compared to TAV controls that varies with the degree of valve stenosis and BAV cusp fusion pattern [9, 40, 43, 49, 59]. This is most pronounced in the mid-ascending aorta [50], where aneurysms are commonly found. Some correlation has also been made between WSS and ascending aorta diameter [50]. Along with the findings of flow displacement, these results support a haemodynamic aetiology of BAV aortopathy.

Shan *et al.* found that WSS correlated with the diameter of the mid-ascending aorta for normally functioning BAV and regurgitant BAV. In the stenotic BAV group, there was a positive correlation between WSS and peak aortic valve velocity at the same level of the aorta [50]. In contrast, Piatti *et al.* [60] did not find a positive correlation between WSS and aortic diameter in patients with normally functioning BAV and with normal size aortas, during a follow-up period of 3 years. However, their study had a short follow-up period and included only 5 patients, so the findings may simply reflect anatomical remodelling occurring at different rates and different time points. Conversely, it may simply reflect the inadequacy of relating WSS with only 1 geometric measurement to explain aneurysm formation and evolution.

Most WSS values summarized in Table 2 for normally functioning BAV and diseased BAV were higher than 0.4 N/m^2 but lower than 1.5 N/m^2, i.e. higher than the atherogenic cut-off for WSS but not high enough to offer protection from endothelial damage. Calculated WSS for healthy volunteers with TAV, on the other hand, were found to be closer to the deleterious cut-off of 0.4 N/m^2, especially in the series of Shan *et al.* [50]. The WSS values calculated for the stenotic BAV by our group were in the atheroprotective range [47]. This discrepancy is likely to have several explanations. Firstly, the cut-off values of WSS quoted by Malek *et al.* [54] pertain to atherosclerosis specifically, whereas studies investigating BAV aortopathy refer to aneurysms. Secondly, the vascular models from which Malek *et al.* derive their numbers based on smaller vessels and typically at bifurcations. Thirdly, the WSS cut-offs for atheroprotective or deleterious effects were derived from direct measurements of WSS in vascular beds and computer simulations (CFD), whereas the other values are calculated from 4D flow MRI data [33, 50, 53, 55] or MR angiography and CFD [47]. Finally, a large discrepancy was found between the WSS values derived from CFD compared to 4D flow MRI by a factor of 2 for healthy TAV and a factor of 6–8 for diseased BAV (Table 2). This may be explained by the fact that 4D flow MRI is known to underestimate WSS [32]. The results by Vergara *et al.* [52] show an even larger discrepancy in WSS. This is due to a different technique of anatomical modelling and application of boundary conditions compared to our group. This highlights the need for both intra- and inter-modality validation.

Statistical analysis

It is not possible to carry out a meaningful statistical analysis of the findings of these studies. The studies are heterogeneous, the methodology is varied and some include a small number of patients. The impact of varied methodology on calculating WSS is discussed above. Data on blood flow pattern, flow displacement, flow angle, COA and helicity are missing from several papers and, therefore, does not allow a meaningful analysis. Consequently, this review does not contain a statistical analysis, and the results presented herein must, therefore, be interpreted with caution. Once again, this highlights the need for a standardized and validated method of measuring and calculating haemodynamic parameters.

CONCLUSION

In conclusion, MRI and CFD allow for direct visualization of blood flow and subsequent calculation of haemodynamic parameters, which demonstrate the consequences of altered aortic valve geometry on downstream blood flow and its effect on

the aorta. Given that WSS explains the effect of a fluid on a tubular vascular structure, it should be the haemodynamic variable of focused investigations to explain aneurysm formation and evolution. This may help formulate new guidelines for diagnosis, monitoring, timing and type of surgery required for each type of BAV morphology and aortopathy phenotype. However, a standardized method of calculating WSS needs to be agreed upon to set reference values and enable predictions on disease progression and management.

Conflict of interest: none declared.

REFERENCES

[1] Michelena HI, Khanna AD, Mahoney D, Margaryan E, Topilsky Y, Suri RM *et al*. Incidence of aortic complications in patients with bicuspid aortic valves. JAMA 2011;306:1104–12.

[2] Verma S, Yanagawa B, Kalra S, Ruel M, Peterson MD, Yamashita MH *et al*. Knowledge, attitudes, and practice patterns in surgical management of bicuspid aortopathy: a survey of 100 cardiac surgeons. J Thorac Cardiovasc Surg 2013;146:1033–40.e4.

[3] Hiratzka LF, Bakris GL, Beckman JA, Bersin RM, Carr VF, Casey DE *et al*. 2010 ACCF/AHA/AATS/ACR/ASA/SCA/SCAI/SIR/STS/SVM guidelines for the diagnosis and management of patients with thoracic aortic disease. J Am Coll Cardiol 2010;55:e27–129.

[4] Erbel R, Aboyans V, Boileau C, Bossone E, Bartolomeo RD, Eggebrecht H *et al*. ESC Guidelines on the diagnosis and treatment of aortic diseases. Kardiol Pol 2014;72:1169–252.

[5] Vieira MS, Hussain T, Figueroa CA. Patient-specific image-based computational modeling in congenital heart disease: a clinician perspective. J Cardiol Ther 2015;2:436–48.

[6] Niwa K, Perloff JK, Bhuta SM, Laks H, Drinkwater DC, Child JS *et al*. Structural abnormalities of great arterial walls in congenital heart disease: light and electron microscopic analyses. Circulation 2001;103:393–400.

[7] Fedak PW, de Sa MP, Verma S, Nili N, Kazemian P, Butany J *et al*. Vascular matrix remodeling in patients with bicuspid aortic valve malformations: implications for aortic dilatation. J Thorac Cardiovasc Surg 2003;126:797–805.

[8] Atkins SK, Cao K, Rajamannan NM, Sucosky P. Bicuspid aortic valve hemodynamics induces abnormal medial remodeling in the convexity of porcine ascending aortas. Biomech Model Mechanobiol 2014;13:1209–25.

[9] Guzzardi DG, Barker AJ, van Ooij P, Malaisrie SC, Puthumana JJ, Belke DD *et al*. Valve-related hemodynamics mediate human bicuspid aortopathy: insights from wall shear stress mapping. J Am Coll Cardiol 2015;66:892–900.

[10] Abdulkareem N, Smelt J, Jahangiri M. Bicuspid aortic valve aortopathy: genetics, pathophysiology and medical therapy. Interact CardioVasc Thorac Surg 2013;17:554–9.

[11] Yassine NM, Shahram JT, Body SC. Pathogenic mechanisms of bicuspid aortic valve aortopathy. Front Physiol 2017;8:687.

[12] Youssefi P, Sharma R, Figueroa CA, Jahangiri M. Functional assessment of thoracic aortic aneurysms—the future of risk prediction? Br Med Bull 2017;121:61–71.

[13] Markl M, Draney MT, Hope MD, Levin JM, Chan FP, Alley MT *et al*. Time-resolved 3-dimensional velocity mapping in the thoracic aorta: visualization of 3-directional blood flow patterns in healthy volunteers and patients. J Comput Assist Tomogr 2004;28:459–68.

[14] Bammer R, Hope TA, Aksoy M, Alley MT. Time-resolved 3D quantitative flow MRI of the major intracranial vessels: initial experience and comparative evaluation at 1.5T and 3.0T in combination with parallel imaging. Magn Reson Med 2007;57:127–40.

[15] Frydrychowicz A, Berger A, Russe MF, Stalder AF, Harloff A, Dittrich S *et al*. Time-resolved magnetic resonance angiography and flow-sensitive 4-dimensional magnetic resonance imaging at 3 Tesla for blood flow and wall shear stress analysis. J Thorac Cardiovasc Surg 2008;136:400–7.

[16] Fillinger MF, Raghavan ML, Marra SP, Cronenwett JL, Kennedy FE. In vivo analysis of mechanical wall stress and abdominal aortic aneurysm rupture risk. J Vasc Surg 2002;36:589–97.

[17] Fillinger MF, Marra SP, Raghavan ML, Kennedy FE. Prediction of rupture risk in abdominal aortic aneurysm during observation: wall stress versus diameter. J Vasc Surg 2003;37:724–32.

[18] Les AS, Shadden SC, Figueroa CA, Park JM, Tedesco MM, Herfkens RJ *et al*. Quantification of hemodynamics in abdominal aortic aneurysms during rest and exercise using magnetic resonance imaging and computational fluid dynamics. Ann Biomed Eng 2010;38:1288–313.

[19] Li Z, Kleinstreuer C. Blood flow and structure interactions in a stented abdominal aortic aneurysm model. Med Eng Phys 2005;27:369–82.

[20] Taylor CA, Draney MT, Ku JP, Parker D, Steele BN, Wang K *et al*. Predictive medicine: computational techniques in therapeutic decision-making. Comput Aided Surg 1999;4:231–47.

[21] Migliavacca F, Balossino R, Pennati G, Dubini G, Hsia T-Y, de Leval MR *et al*. Multiscale modelling in biofluidynamics: application to reconstructive paediatric cardiac surgery. J Biomech 2006;39:1010–20.

[22] Prasad A, Xiao N, Gong X-Y, Zarins CK, Figueroa CA. A computational framework for investigating the positional stability of aortic endografts. Biomech Model Mechanobiol 2013;12:869–87.

[23] Xiong G, Figueroa CA, Xiao N, Taylor CA. Simulation of blood flow in deformable vessels using subject-specific geometry and spatially varying wall properties. Int J Numer Method Biomed Eng 2011;27:1000–16.

[24] Morris PD, Narracott A, Tengg-Kobligk H, Silva Soto DA, Hsiao S, Lungu A *et al*. Computational fluid dynamics modelling in cardiovascular medicine. Heart 2016;102:18–28.

[25] Steinman DA. Image-based computational fluid dynamics modeling in realistic arterial geometries. Ann Biomed Eng 2002;30:483–97.

[26] Chandran KB, Vigmostad SC. Patient-specific bicuspid valve dynamics: overview of methods and challenges. J Biomech 2013;46:208–16.

[27] Markl M, Schnell S, Wu C, Bollache E, Jarvis K, Barker AJ *et al*. Advanced flow MRI: emerging techniques and applications. Clin Radiol 2016;71:779–95.

[28] Markl M, Harloff A, Bley TA, Zaitsev M, Jung B, Weigang E *et al*. Time-resolved 3D MR velocity mapping at 3T: improved navigator-gated assessment of vascular anatomy and blood flow. J Magn Reson Imaging 2007;25:824–31.

[29] Markl M, Frydrychowicz A, Kozerke S, Hope M, Wieben O. 4D flow MRI. J Magn Reson Imaging 2012;36:1015–36.

[30] Schnell S, Entezari P, Mahadewia RJ, Malaisrie SC, McCarthy PM, Collins JD *et al*. Improved semi-automated 4D-flow MRI analysis in the aorta in patients with congenital aortic valve anomalies vs tricuspid aortic valves. J Comput Assist Tomogr 2016;40:102–8.

[31] Ha H, Kim GB, Kweon J, Lee SJ, Kim Y-H, Lee DH *et al*. Hemodynamic measurement using four-dimensional phase-contrast MRI: quantification of hemodynamic parameters and clinical applications. Korean J Radiol 2016;17:445–62.

[32] Petersson S, Dyverfeldt P, Ebbers T. Assessment of the accuracy of MRI wall shear stress estimation using numerical simulations. J Magn Reson Imaging 2012;36:128–38.

[33] Mahadevia R, Barker AJ, Schnell S, Entezari P, Kansal P, Fedak PWM *et al*. Bicuspid aortic cusp fusion morphology alters aortic 3D outflow patterns, wall shear stress and expression of aortopathy. Circulation 2014;129:673–82.

[34] Hope MD, Hope TA, Meadows AK, Ordovas KG, Urbania TH, Alley MT *et al*. Bicuspid aortic valve: four-dimensional MR evaluation of ascending aortic systolic flow patterns. Radiology 2010;255:53–61.

[35] Kimura N, Nakamura M, Komiya K, Nishi S, Yamaguchi A, Tanaka O *et al*. Patient-specific assessment of hemodynamics by computational fluid dynamics in patients with bicuspid aortopathy. J Thorac Cardiovasc Surg 2017;153:S52–62.

[36] Farthing S, Peronneau P. Flow in the thoracic aorta. Cardiovasc Res 1979;13:607–20.

[37] Kilner PJ, Yang GZ, Mohiaddin RH, Firmin DN, Longmore DB. Helical and retrograde secondary flow patterns in the aortic arch studied by three-directional magnetic resonance velocity mapping. Circulation 1993;88:2235–47.

[38] Bissell MM, Hess AT, Biasiolli L, Glaze SJ, Loudon M, Pitcher A *et al*. Aortic dilation in bicuspid aortic valve disease: flow pattern is a major contributor and differs with valve fusion type. Circ Cardiovasc Imaging 2013;6:499–507.

[39] Garcia J, Barker AJ, Murphy I, Jarvis K, Schnell S, Collins JD *et al*. Four-dimensional flow magnetic resonance imaging-based characterization of aortic morphometry and haemodynamics: impact of age, aortic diameter, and valve morphology. Eur Heart J Cardiovasc Imaging 2016;17:877–84.

[40] Sigovan M, Hope MD, Dyverfeldt P, Saloner D. Comparison of four-dimensional flow parameters for quantification of flow eccentricity in the ascending aorta. J Magn Reson Imaging 2011;34:1226–30.
[41] Raghav V, Barker AJ, Mangiameli D, Mirabella L, Markl M, Yoganathan AP. Valve mediated hemodynamics and their association with distal ascending aortic diameter in bicuspid aortic valve subjects. J Magn Reson Imaging 2018;47:246–54.
[42] Della Corte A, Bancone C, Dialetto G, Covino FE, Manduca S, D'Oria V *et al*. Towards an individualized approach to bicuspid aortopathy: different valve types have unique determinants of aortic dilatation. Eur J Cardiothorac Surg 2014;45:e118–24.
[43] Burris NS, Hope MD. Bicuspid valve-related aortic disease: flow assessment with conventional phase-contrast MRI. Acad Radiol 2015;22:690.
[44] Della Corte A, Bancone C, Conti CA, Votta E, Redaelli A, Del Viscovo L *et al*. Restricted cusp motion in right-left type of bicuspid aortic valves: a new risk marker for aortopathy. J Thorac Cardiovasc Surg 2012;144:360–9.
[45] Hardman D, Semple SI, Richards JMJ, Hoskins PR. Comparison of patient-specific inlet boundary conditions in the numerical modelling of blood flow in abdominal aortic aneurysm disease. Int J Numer Method Biomed Eng 2013;29:165–78.
[46] Cao K, Atkins SK, McNally A, Liu J, Sucosky P. Simulations of morphotype-dependent hemodynamics in non-dilated bicuspid aortic valve aortas. J Biomech 2017;50:63–70.
[47] Youssefi P, Gomez A, He T, Anderson L, Bunce N, Sharma R *et al*. Patient-specific computational fluid dynamics—assessment of aortic hemodynamics in a spectrum of aortic valve pathologies. J Thorac Cardiovasc Surg 2017;153:8–20.
[48] Della Corte A, de Santo L, Montagnani S, Quarto C, Romano G, Amarelli C *et al*. Spatial patterns of matrix protein expression in dilated ascending aorta with aortic regurgitation: congenital bicuspid valve versus Marfan's syndrome. J Heart Valve Dis 2006;15:20–7.
[49] Verma S, Siu SC. Aortic dilatation in patients with bicuspid aortic valve. N Engl J Med 2014;370:1920–9.
[50] Shan Y, Li J, Wang Y, Wu B, Barker AJ, Markl M *et al*. Aortic shear stress in patients with bicuspid aortic valve with stenosis and insufficiency. J Thorac Cardiovasc Surg 2017;153:1263–72.
[51] Hope MD, Hope TA, Crook SE, Ordovas KG, Urbania TH, Alley MT *et al*. 4D flow CMR in assessment of valve-related ascending aortic disease. JACC Cardiovasc Imaging 2011;4:781.
[52] Vergara C, Viscardi F, Antiga L, Luciani GB. Influence of bicuspid valve geometry on ascending aortic fluid dynamics: a parametric study. Artif Organs 2012;36:368–78.
[53] van Ooij P, van Markl M, Collins JD, Carr JC, Rigsby C, Bonow RO *et al*. Aortic valve stenosis alters expression of regional aortic wall shear stress: new insights from a 4-dimensional flow magnetic resonance imaging study of 571 subjects. J Am Heart Assoc 2017;6:e005959.
[54] Malek AM, Alper SL, Izumo S. Hemodynamic shear stress and its role in atherosclerosis. JAMA 1999;282:2035–42.
[55] Meierhofer C, Schneider EP, Lyko C, Hutter A, Martinoff S, Markl M *et al*. Wall shear stress and flow patterns in the ascending aorta in patients with bicuspid aortic valves differ significantly from tricuspid aortic valves: a prospective study. Eur Heart J Cardiovasc Imaging 2013;14:797–804.
[56] Cebral JR, Vazquez M, Sforza DM, Houzeaux G, Tateshima S, Scrivano E *et al*. Analysis of hemodynamics and wall mechanics at sites of cerebral aneurysm rupture. J Neurointerv Surg 2015;7:530–6.
[57] Fedak PWM, Barker AJ, Verma S. Year in review: bicuspid aortopathy. Curr Opin Cardiol 2016;31:132–8.
[58] Kontopodis N, Pantidis D, Dedes A, Daskalakis N, Ioannou CV. The—not so—solid 5.5 cm threshold for abdominal aortic aneurysm repair: facts, misinterpretations, and future directions. Front Surg 2016;3:1.
[59] Barker AJ, Markl M, Bürk J, Lorenz R, Bock J, Bauer S *et al*. Bicuspid aortic valve is associated with altered wall shear stress in the ascending aorta. Circ Cardiovasc Imaging 2012;5:457–66.
[60] Piatti F, Sturla F, Bissell MM, Pirola S, Lombardi M, Nesteruk I *et al*. 4D flow analysis of BAV-related fluid-dynamic alterations: evidences of wall shear stress alterations in absence of clinically-relevant aortic anatomical remodeling. Front Physiol 2017;8:441.